

## Tetrahedral-Site Occupancies in Sodium Aluminum-Gallium Feldspar Solid Solutions [Na(Al<sub>1-x</sub>Ga<sub>x</sub>)Si<sub>3</sub>O<sub>8</sub>]

MICHAEL E. FLEET

*Department of Geology, University of Western Ontario, London, Ontario, Canada N6A 5B7*

Received October 10, 1990

The structures of two sodium aluminum-gallium feldspars [Na(Al<sub>1-x</sub>Ga<sub>x</sub>)Si<sub>3</sub>O<sub>8</sub>] have been synthesized hydrothermally, and refined at room temperature with single-crystal X-ray intensities. Tetrahedral-site occupancies for gallium have been obtained by direct refinement and for aluminum by analysis of partial T–O distances ( $T = \text{Si, Al, Ga}$ ). For  $x = 0.1$ , 630°C, 1.3 kbar,  $R = 0.031$ , gallium occupancies for the four tetrahedral positions are  $t_10 = 0.070$ ,  $t_1m = 0.000(1)$ ,  $t_20 = 0.014(1)$ ,  $t_2m = 0.014(1)$ , and aluminum occupancies are 0.35, 0.19, 0.18, 0.18, respectively. For  $x = 0.3$ , 631°C, 1.3 kbar,  $R = 0.032$ , gallium occupancies are  $t_10 = 0.168$ ,  $t_1m = 0.016(1)$ ,  $t_20 = 0.053(1)$ ,  $t_2m = 0.063(1)$ , and aluminum occupancies are 0.27, 0.13, 0.14, 0.15, respectively. The site preference of gallium is not significantly modified by change in the extended feldspar structure; gallium remains largely ordered with the site preference sequence  $t_10 \gg t_20 \approx t_2m > t_1m \rightarrow 0.0$ . It does not appear that the ordering of gallium is influenced to any significant degree at the experimental temperatures by coupling with the lattice strain of the disordered host crystal. © 1991 Academic Press, Inc.

### Introduction

In recent studies (1, 2), the substitution of gallium and germanium into the structure of sodium feldspar (NaAlSi<sub>3</sub>O<sub>8</sub>) was used as an additional (chemical) dimension in the study of order–disorder in alkali feldspar. The structures of triclinic alkali feldspars (space group  $C\bar{1}$ ) have four nonequivalent tetrahedral sites for silicon and aluminum, designated by  $T_10$ ,  $T_1m$ ,  $T_20$ , and  $T_2m$ , with occupancies of aluminum (or trivalent atoms) designated by  $t_10$ ,  $t_1m$ ,  $t_20$ , and  $t_2m$ , respectively [e.g., (3)]. The study of the ordering of aluminum and silicon among these tetrahedral sites is complicated by the sluggishness of the ordering process and small differences in X-ray scattering efficiencies of aluminum and silicon. Throughout this

paper, “albite” is sodium feldspar, “gallium albite” is synthetic NaGaSi<sub>3</sub>O<sub>8</sub> with the albite structure, “low albite” has a largely ordered structure, and “high albite” has a largely disordered structure.

As reviewed in Fleet (2), tetrahedral-site ordering closely approximates to  $t_10 > t_1m \approx t_20 \approx t_2m < 0.25$  in high albite [e.g., (4, 5)],  $t_10 \rightarrow 1$ ,  $t_1m \approx t_20 \approx t_2m \rightarrow 0$  in low albite [e.g., (5–8)], and  $t_10 \rightarrow 1$ ,  $t_1m \geq t_20 \approx t_2m \rightarrow 0$  in triclinic K-rich feldspars (5, 8).

There have been several X-ray powder and single-crystal studies on gallium-substituted sodium feldspar (1, 2, 9–11). The order–disorder transformation in gallium albite is continuous (1) with a well-defined region of intermediate structure and an ordering path of  $t_10 \rightarrow 1$ ,  $t_1m \approx t_20 \approx t_2m \rightarrow 0$ , with some tendency for  $t_2m \neq t_20$ . Fleet (2)

investigated the crystal structure of low gallium albite, synthesized hydrothermally at 600°C, 1.3 kbar, and reported gallium occupancies of  $t_10 = 0.935$ ,  $t_1m = 0.016$ ,  $t_20 = 0.025$ ,  $t_2m = 0.025$ .

The behavior of gallium in aluminum-gallium albite solid solutions, and particularly within a matrix of (disordered) high albite structure, is of interest because of the possibility of the high albite-type lattice inducing disorder in the distribution of gallium, and to further understand the controls on order-disorder of tetrahedral cations in alkali feldspars. The present paper reports on tetrahedral-site occupancies in two aluminum-gallium albites with about 10 and 30 mole% NaGaSi<sub>3</sub>O<sub>8</sub>. Gallium occupancies are obtained by direct X-ray structure refinement, making use of the large difference in X-ray scattering efficiency between gallium and aluminum/silicon. Aluminum occupancies are deduced from analysis of partial tetrahedral bond distances, and silicon occupancies are obtained by difference.

### Experimental Procedures

Single crystals with about 10 and 30 mole% NaGaSi<sub>3</sub>O<sub>8</sub> (hereafter referred to as Al90Ga10 and Al70Ga30, respectively) were grown from a melt using a standard cold-seal hydrothermal reaction vessel. Starting materials were in the form of glasses of nominal composition Al90Ga10 and Al50Ga50, respectively, and prepared from purified Ga<sub>2</sub>O<sub>3</sub> and SiO<sub>2</sub> and analytical grade Na<sub>2</sub>CO<sub>3</sub>. Charges consisted of 0.065 g of glass, 0.05 g of Na<sub>2</sub>CO<sub>3</sub>, and 0.02 cm<sup>3</sup> of deionized water contained in a sealed gold capsule about 4 cm in length. They were heated to 840–850°C at 2 kbar for 1 hr, cooled stepwise, and maintained at about 650°C overnight, and then cooled further stepwise and maintained at 630°C, 1.3 kbar for 10 days for Al90Ga10 and 631°C, 1.3 kbar for 9 days for Al70Ga30, and quenched in air and water. By electron mi-

croprobe analysis, the crystals used for reflection intensities were essentially homogeneous (for Al90Ga10, the variation in Ga<sub>2</sub>O<sub>3</sub> was from 2.94 to 3.97 wt%, and, for Al70Ga30, it was from 9.45 to 11.16 wt%), and contained 9.8 and 30.1 mole% NaGaSi<sub>3</sub>O<sub>8</sub>, respectively.

All single-crystal measurements, made with an Enraf-Nonius CAD-4F diffractometer and graphite-monochromatized MoK $\alpha$  X-radiation, and structure refinements closely followed earlier procedures for gallium albite (2). Both single crystals investigated had about 0.5% of an albite-twin component (3), which was ignored. Intensity data were collected in the  $\omega$  scan mode. Scattering factors for neutral atomic species and  $f'$ ,  $f''$  were taken from Ref. (12). All computations were carried out with DATAP77 and LINEX77 (State University of New York at Buffalo). Further experimental details are given below, and the results are summarized in Tables I–V.<sup>1</sup>

*Al90Ga10*. Unit-cell parameters are  $a = 8.149(3)$ ,  $b = 12.870(2)$ ,  $c = 7.127(2)$  Å,  $\alpha = 93.76(2)$ ,  $\beta = 116.48(2)$ ,  $\gamma = 89.75(2)^\circ$ ,  $V = 667.3$  Å<sup>3</sup>; 3891 reflections out to  $2\theta = 60^\circ$  were measured. Transmission factors varied from 0.797 for 0,  $-2$ , 0 to 0.848 for  $-5$ ,  $-1$ , 10 (crystal volume =  $3.35 \times 10^{-3}$  mm<sup>3</sup>,  $\mu = 13.3$  cm<sup>-1</sup>). There were 1946 unique reflections, with 395 considered unobserved on the basis of  $I < 3\sigma(I)$ . Refinement in  $C\bar{1}$  used weighted averaged scattering factors for aluminum and silicon, and

<sup>1</sup> See NAPS document No. 04843 for 28 pages of supplementary material. Order from ASIS/NAPS, Microfiche Publications, P.O. Box 3513, Grand Central Station, New York, NY 10163. Remit in advance \$4.00 for microfiche copy or for photocopy, \$7.75 up to 20 pages plus \$.30 for each additional page. All orders must be prepaid. Institutions and Organizations may order by purchase order. However, there is a billing and handling charge for this service of \$15. Foreign orders add \$4.50 for postage and handling, for the first 20 pages, and \$1.00 for additional 10 pages of material, \$1.50 for postage of any microfiche orders.

TABLE I  
POSITIONAL AND ISOTROPIC THERMAL PARAMETERS  
( $\text{\AA}^2$ )  $B_{\text{eq}} = \frac{1}{3} \sum_i \sum_j \beta_{ij} a_i \cdot a_j$

|   | <i>x</i>  | <i>y</i>  | <i>z</i>  | $B_{\text{eq}}$ |
|---|-----------|-----------|-----------|-----------------|
| Al90Ga10, 10 mole% NaGaSi <sub>3</sub> O <sub>8</sub> |           |           |           |                 |
| Na  | 0.2727(2) | 0.0036(2) | 0.1366(3) | 7.20(7)         |
| T <sub>1</sub> 0                                      | 0.0085(1) | 0.1656(1) | 0.2130(1) | 1.02(1)         |
| T <sub>1</sub> <i>m</i>                               | 0.0043(1) | 0.8153(1) | 0.2306(1) | 0.74(1)         |
| T <sub>2</sub> 0                                      | 0.6906(1) | 0.1082(1) | 0.3187(1) | 0.77(1)         |
| T <sub>2</sub> <i>m</i>                               | 0.6838(1) | 0.8783(1) | 0.3551(1) | 0.74(1)         |
| O <sub>A</sub> 1                                      | 0.0056(3) | 0.1343(2) | 0.9801(3) | 1.64(5)         |
| O <sub>A</sub> 2                                      | 0.5920(2) | 0.9918(1) | 0.2791(3) | 1.27(5)         |
| O <sub>B</sub> 0                                      | 0.8192(3) | 0.1079(2) | 0.1963(3) | 1.67(5)         |
| O <sub>B</sub> <i>m</i>                               | 0.8184(3) | 0.8469(2) | 0.2487(3) | 1.85(5)         |
| O <sub>C</sub> 0                                      | 0.0151(3) | 0.2924(1) | 0.2763(3) | 1.55(5)         |
| O <sub>C</sub> <i>m</i>                               | 0.0223(3) | 0.6882(1) | 0.2200(3) | 1.53(5)         |
| O <sub>D</sub> 0                                      | 0.1985(3) | 0.1115(1) | 0.3878(3) | 1.46(5)         |
| O <sub>D</sub> <i>m</i>                               | 0.1868(3) | 0.8672(2) | 0.4295(3) | 1.65(5)         |
| Al70Ga30, 30 mole% NaGaSi <sub>3</sub> O <sub>8</sub> |           |           |           |                 |
| Na  | 0.2729(2) | 0.0024(2) | 0.1379(3) | 7.37(7)         |
| T <sub>1</sub> 0                                      | 0.0080(1) | 0.1662(1) | 0.2115(2) | 0.98(2)         |
| T <sub>1</sub> <i>m</i>                               | 0.0038(1) | 0.8155(1) | 0.2313(1) | 0.75(1)         |
| T <sub>2</sub> 0                                      | 0.6910(1) | 0.1084(1) | 0.3178(1) | 0.79(2)         |
| T <sub>2</sub> <i>m</i>                               | 0.6832(1) | 0.8785(1) | 0.3559(1) | 0.76(2)         |
| O <sub>A</sub> 1                                      | 0.0058(3) | 0.1342(2) | 0.9776(4) | 1.80(6)         |
| O <sub>A</sub> 2                                      | 0.5916(3) | 0.9924(2) | 0.2792(3) | 1.40(5)         |
| O <sub>B</sub> 0                                      | 0.8186(3) | 0.1076(2) | 0.1930(4) | 1.79(6)         |
| O <sub>B</sub> <i>m</i>                               | 0.8188(3) | 0.8465(2) | 0.2497(4) | 1.99(6)         |
| O <sub>C</sub> 0                                      | 0.0145(3) | 0.2932(2) | 0.2766(3) | 1.73(6)         |
| O <sub>C</sub> <i>m</i>                               | 0.0226(3) | 0.6890(2) | 0.2200(3) | 1.66(6)         |
| O <sub>D</sub> 0                                      | 0.1997(3) | 0.1112(2) | 0.3862(3) | 1.53(6)         |
| O <sub>D</sub> <i>m</i>                               | 0.1852(3) | 0.8669(2) | 0.4308(3) | 1.80(6)         |

converged to  $R = 0.031$ ,  $R_w = 0.029$  [for reflections with  $I \geq 3\sigma(I)$ ,  $S = 1.618$ ,  $g = 0.09(2) \times 10^{-4}$ ,  $\Delta\rho = -0.70$  to  $0.63 \text{ e\AA}^{-3}$  (both near Na)].

*Al70Ga30*. Unit-cell parameters are  $a = 8.173(2)$ ,  $b = 12.874(2)$ ,  $c = 7.130(2) \text{ \AA}$ ,  $\alpha = 93.86(2)$ ,  $\beta = 116.48(2)$ ,  $\gamma = 89.52(2)^\circ$ ,  $V = 669.8 \text{ \AA}^3$ ; 3898 reflections out to  $2\theta = 60^\circ$  were measured. Transmission factors varied from 0.726 for 0, -2, 0 to 0.869 for 2, 0, 2 (crystal volume =  $1.54 \times 10^{-3} \text{ mm}^3$ ,  $\mu = 21.3 \text{ cm}^{-1}$ ). There were 1949 unique reflections, with 528 considered unobserved on the basis of  $I < 3\sigma(I)$ . Refinement in  $C\bar{1}$  used weighted averaged scattering factors for aluminum and silicon, and converged to  $R = 0.032$ ,  $R_w = 0.029$  [for reflections with  $I \geq 3\sigma(I)$ ,  $S = 1.259$ ,  $g = 0.02(3) \times 10^{-4}$ ,  $\Delta\rho = -0.68$  to  $0.59 \text{ e\AA}^{-3}$  (both near Na)].

## Results and Discussion

*Tetrahedral-site occupancies*. Direct refinement of the tetrahedral-site occupancies of gallium [ $t_i(\text{Ga})$ , Table III] was facilitated by the appreciably greater X-ray scattering efficiency of gallium ( $Z = 31$ ) compared to aluminum and silicon ( $Z = 13$  and  $14$ , respectively).  $T_1$ 0-site occupancies were obtained by difference ( $t_1m + t_20 + t_2m$ ) from 0.098 for Al90Ga10 and from 0.300 for

TABLE II  
TETRAHEDRAL (T-O) BOND DISTANCES ( $\text{\AA}$ )

|   | Al90Ga10 | Al70Ga30 |   | Al90Ga10 | Al70Ga30 |
|---|----------|----------|---|----------|----------|
| $T_1$ 0-O <sub>A</sub> 1                | 1.672(2) | 1.683(2) | $T_2$ 0-O <sub>A</sub> 2                | 1.651(2) | 1.652(2) |
| $T_1$ 0-O <sub>B</sub> 0                | 1.667(1) | 1.675(2) | $T_2$ 0-O <sub>B</sub> 0                | 1.635(2) | 1.645(2) |
| $T_1$ 0-O <sub>C</sub> 0                | 1.659(2) | 1.665(2) | $T_2$ 0-O <sub>C</sub> <i>m</i>         | 1.630(1) | 1.636(2) |
| $T_1$ 0-O <sub>D</sub> 0                | 1.679(1) | 1.693(2) | $T_2$ 0-O <sub>D</sub> <i>m</i>         | 1.627(2) | 1.628(2) |
| Average                                 | 1.669    | 1.679    | Average                                 | 1.636    | 1.640    |
| $T_1$ <i>m</i> -O <sub>A</sub> 1        | 1.644(2) | 1.633(2) | $T_2$ <i>m</i> -O <sub>A</sub> 2        | 1.650(2) | 1.654(2) |
| $T_1$ <i>m</i> -O <sub>B</sub> <i>m</i> | 1.624(1) | 1.619(2) | $T_2$ <i>m</i> -O <sub>B</sub> <i>m</i> | 1.624(2) | 1.634(2) |
| $T_1$ <i>m</i> -O <sub>C</sub> <i>m</i> | 1.641(2) | 1.634(2) | $T_2$ <i>m</i> -O <sub>C</sub> 0        | 1.634(1) | 1.635(2) |
| $T_1$ <i>m</i> -O <sub>D</sub> <i>m</i> | 1.635(1) | 1.634(2) | $T_2$ <i>m</i> -O <sub>D</sub> 0        | 1.642(2) | 1.648(2) |
| Average                                 | 1.636    | 1.630    | Average                                 | 1.637    | 1.643    |

TABLE III  
TETRAHEDRAL-SITE OCCUPANCIES ( $t_i$ ) AND  $T$ -O BOND DISTANCES (Å)

| Site  | $t_i(\text{Ga})$ |                 | $T$ -O<br>3 | Ga-O<br>partial<br>4 | Al, Si-O<br>normalized<br>5 | $T$ -O<br>high albite<br>6 | $t_i(\text{Å})$<br>normalized<br>7 | $t_i$<br>(Al)<br>8 | $t_i$<br>(Si)<br>9 |
|---|------------------|-----------------|-------------|----------------------|-----------------------------|----------------------------|------------------------------------|--------------------|--------------------|
|   | Refined<br>1     | Normalized<br>2 |             |                      |                             |                            |                                    |                    |                    |
| Al90Ga10, 10 mole% NaGaSi <sub>3</sub> O <sub>8</sub> |                  |                 |             |                      |                             |                            |                                    |                    |                    |
| $T_10$  | 0.070            | 0.712           | 1.669       | 0.126                | 1.659                       | 1.646                      | 0.39                               | 0.35               | 0.58               |
| $T_1m$  | 0.000(1)         | 0.004           | 1.636       | 0.000                | 1.636                       | 1.641                      | 0.21                               | 0.19               | 0.81               |
| $T_20$  | 0.014(1)         | 0.139           | 1.636       | 0.025                | 1.634                       | 1.641                      | 0.20                               | 0.18               | 0.81               |
| $T_2m$  | 0.014(1)         | 0.145           | 1.637       | 0.025                | 1.635                       | 1.642                      | 0.20                               | 0.18               | 0.81               |
| Al70Ga30, 30 mole% NaGaSi <sub>3</sub> O <sub>8</sub> |                  |                 |             |                      |                             |                            |                                    |                    |                    |
| $T_10$  | 0.168            | 0.558           | 1.679       | 0.304                | 1.653                       | 1.646                      | 0.38                               | 0.27               | 0.57               |
| $T_1m$  | 0.016(1)         | 0.055           | 1.630       | 0.029                | 1.627                       | 1.641                      | 0.18                               | 0.13               | 0.86               |
| $T_20$  | 0.053(1)         | 0.177           | 1.640       | 0.096                | 1.630                       | 1.641                      | 0.20                               | 0.14               | 0.81               |
| $T_2m$  | 0.063(1)         | 0.211           | 1.643       | 0.114                | 1.632                       | 1.642                      | 0.22                               | 0.15               | 0.78               |

Note. 1, By direct refinement; 2, normalized to  $\sum t_i = 1.0$ ; 3, Table II; 4,  $t_i(\text{Ga}) \times 1.807 \text{ Å}$ ; 5, derived from columns 1, 3, and 4, on Ga-free basis; 6, (13); 7, derived using  $t_i = 0.25 - (\langle T_1\text{-O} \rangle - \langle T_2\text{-O} \rangle)/0.130$  (8) and column 5.

Al70Ga30. In Al90Ga10, gallium is strongly partitioned into  $T_10$ . Relative gallium site occupancies are  $t_{10} \gg t_{20} \approx t_{2m} > t_{1m} = 0.0$ , and the normalized occupancies for equivalent end-member NaGaSi<sub>3</sub>O<sub>8</sub> composition (Table III) correspond to a low gallium albite configuration. In Al70Ga30, gallium again favors  $T_10$ , with relative gallium site occupancies of  $t_{10} > t_{20} \approx t_{2m} > t_{1m}$ . However, the normalized occupancies now correspond to an intermediate ordered configuration. These results are consistent with the ordering observed in low gallium albite (2) and confirm the strong preference of gallium for  $T_10$ , the subordinate and approximately equal preference of gallium for  $T_20$  and  $T_2m$ , and the lack of preference of gallium for  $T_1m$ . The latter feature was not observed in the Rietveld refinements of transformed gallium albite (1) and, in this respect, the intermediate ordered configuration of Al70Ga30 does not correspond to the intermediate ordered gallium albite recognized in the earlier study. The weaker

preference of gallium for  $T_1m$  compared to  $T_20$  and  $T_2m$ , which characterizes the single-crystal X-ray structure refinements, is in marked contrast to the one-step ordering of albite (cf. 5), for which  $t_{10} > t_{1m} \approx t_{20} \approx t_{2m}$ .

It is well known that tetrahedral ( $T$ -O) bond lengths in aluminosilicate alkali feldspars primarily reflect tetrahedral-site occupancies [e.g., (8)]. Average  $T$ -O distances (Table II) for Al90Ga10 and Al70Ga30 are in good qualitative agreement with the refined gallium occupancies,  $\langle T_10\text{-O} \rangle$  being appreciably larger than the other average distances ( $\langle T_1m\text{-O} \rangle$ ,  $\langle T_20\text{-O} \rangle$ , and  $\langle T_2m\text{-O} \rangle$ ), which, in turn, are similar to the corresponding average distances in high albite (13).

Further analysis of the average tetrahedral bond distances, assuming that the contributions of the individual Al-O, Ga-O, and Si-O distances (hereafter referred to as *partial*  $T$ -O distances) may be summed linearly, allows aluminum site occupancies to

be deduced and suggests fairly precise agreement with both the refined gallium occupancies and the  $t_1(\text{Al})$  vs  $\langle T_1\text{-O} \rangle$  relationship of Kroll and Ribbe (8). Partial Ga–O distances (column 4 of Table III) have been obtained from the product of  $t_1(\text{Ga})$  and 1.807 Å [the average  $T_1\text{-O}$  distance of low gallium albite (2) not corrected for site-to-site variation attributable to stereochemical effects]. Subtraction of the partial Ga–O distances from the observed average distances ( $\langle T\text{-O} \rangle$ ), with normalization to end-member composition, yielded the normalized Al, Si–O distances of column 5 (Table III). These were used to derive  $t_1(\text{Al})$  from the formula of Kroll and Ribbe [(8), given in the footnote to Table III].

Relative to this formula, the high albite of Prewitt *et al.* (13) is almost completely disordered ( $t_{10} = 0.273$ ). Thus, qualitative comparison of columns 5 and 6 of Table III clearly indicates a higher degree of order of the aluminum/silicon distribution in both  $\text{Al}_{90}\text{Ga}_{10}$  and  $\text{Al}_{70}\text{Ga}_{30}$  than in the high albite of Prewitt *et al.* (13). In fact, the normalized aluminum occupancies in the two present structures are very similar (identical within error of calculation), and are precisely consistent with a one-step ordering model ( $t_{10} > t_{1m} \approx t_{20} \approx t_{2m}$ ).

*Sodium feldspar solid solutions and controls on ordering.* In the two sodium aluminum-gallium feldspars (albite) investigated, gallium remains ordered within a matrix of high albite structure. These solid solutions are basically mixtures of high aluminum/silicon and low or low-intermediate gallium/silicon configurations. Compared to the structure of gallium albite at the same temperature, the site preference of gallium in dilute solution is not significantly modified by change in the extended feldspar structure. Site preference is determined largely by the stereochemical association with nearest-neighboring (oxygen) atoms. The effects of next-nearest neighbors (Si, Al, Ga) and small changes in oxy-

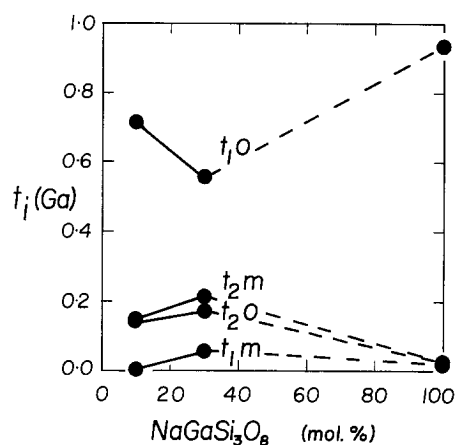


FIG. 1. Normalized gallium occupancies [ $t_i(\text{Ga})$ ] in sodium aluminum-gallium feldspars ( $\text{Al}_{90}\text{Ga}_{10}$ ,  $\text{Al}_{70}\text{Ga}_{30}$ ) compared with low gallium albite [ $\text{NaGaSi}_3\text{O}_8$ ; (2)], illustrating the trend toward intermediate ordered states.

gen bond angles must be of subordinate importance. However, there is a tendency for the aluminum/silicon and gallium/silicon ordering to approach intermediate configurations, particularly at 30 mole%  $\text{NaGaSi}_3\text{O}_8$  (Fig. 1, Table III), and this is evidence for cooperative mixing effects.

Sajje (14) has emphasized the importance of lattice strain in inducing order-disorder in sodium feldspar. For the present aluminum-gallium feldspar solid solutions, however, it does not appear that the ordering of gallium is influenced to any significant degree at the experimental temperature (about 630°C) by coupling with the lattice strain of the disordered host crystal.

The present results for major amounts of gallium in albite may be compared with the behavior of minor and trace amounts of ferric iron in albite (15). By electron paramagnetic resonance spectroscopy,  $\text{Fe}^{3+}$  remained exclusively in the  $T_{10}$  site when natural albite was incipiently disordered by annealing. The tetrahedral-site preference of  $\text{Fe}^{3+}$  at higher degrees of aluminum/silicon disorder and higher concentrations of

iron is unknown, but in light of the present study would be of considerable interest. Ferric iron is disordered over  $T_1$  and  $T_2$  sites in sanidine [disordered  $\text{KAlSi}_3\text{O}_8$ , (16)] and ordered on the  $T_10$  site in microcline [ordered  $\text{KAlSi}_3\text{O}_8$ , (17)]. Fleet (2) surmised that the  $T_10$  site preference for trivalent cations in sodium feldspar decreases in the sequence  $\text{Fe}^{3+} > \text{Ga} > \text{B} > \text{Al}$ , but this might have to be revised if trace and minor amounts of  $\text{Fe}^{3+}$  were disordered in a high albite matrix. However, the present study has not investigated the site preference of trace and minor levels of gallium. This could be quite different to that exhibited by 10 and 30 mole% solid solutions.

Fleet (2) tentatively concluded that the ordering scheme for Si, Al, Ga, Ge, B, and  $\text{Fe}^{3+}$  in sodium feldspar is determined by the favorable charge balance or valence electron distribution resulting when the trivalent cation is placed in the  $T_10$  site. The present structural refinements do reveal a marked difference in the preference of gallium for  $T_1m$  compared to  $T_20$  and  $T_2m$ , but opposite to that predicted (2) from the hypothetical charge-balancing role of the oxygen atom  $\text{O}_A1$ ; that is, in sodium aluminum-gallium feldspar solid solutions, silicon exhibits a weak preference for  $T_1m$ . However, this could be a consequence of an additional factor associated with the disordered matrix promoting the preference of gallium for  $T_20$  and  $T_2m$ . One final point, if next-nearest-neighboring tetrahedral cations were a significant factor in determining site preference in alkali feldspars, in ordered albite structures, silicon would exhibit a stronger preference for  $T_2m$ , which

has two next-nearest-neighbor trivalent cations, than  $T_20$ .

### Acknowledgments

I thank Y. Pan for electron microprobe analyses, and the Natural Sciences and Engineering Research Council of Canada for financial support.

### References

1. P. C. BURNS AND M. E. FLEET, *Phys. Chem. Miner.* **17**, 108 (1990).
2. M. E. FLEET, *Am. Mineral.*, in press (1991).
3. J. V. SMITH, "Feldspar Minerals," Vol. 1, Springer-Verlag, Berlin (1974).
4. P. H. RIBBE, H. D. MEGAW, W. H. TAYLOR, R. B. FERGUSON, AND R. J. TRAILL, *Acta Crystallogr. Sect. B* **25**, 1503 (1969).
5. J. V. SMITH AND W. L. BROWN, "Feldspar Minerals," Vol. 1, 2nd ed., Springer-Verlag, Berlin (1988).
6. G. E. HARLOW AND G. E. BROWN, JR., *Am. Mineral.* **65**, 986 (1980).
7. M. W. PHILLIPS, P. H. RIBBE, AND A. A. PINKERTON, *Acta Crystallogr. Sect. C* **45**, 542 (1989).
8. H. KROLL AND P. H. RIBBE, *Am. Mineral.* **72**, 491 (1987).
9. H. PENTINGHAUS, Dissertation, Universitat Munster (1970).
10. H. PENTINGHAUS AND H. H. STEUHL, *Fortschr. Min.* (Beiheft 1) **49**, 38 (1971).
11. D. K. SWANSON, Ph.D. thesis, State University NY, Stony Brook (1986).
12. J. A. IBERS AND W. C. HAMILTON, Eds. "International Tables for X-Ray Crystallography," Vol. IV, Kynoch, Birmingham, England (1974).
13. C. T. PREWITT, S. SUENO, AND J. J. PAPIKE, *Am. Mineral.* **61**, 1213 (1976).
14. E. SALJE, *Phys. Chem. Miner.* **12**, 93 (1985).
15. I. PETROV., F. YUDE, L. V. BERSHOV, S. S. HAFNER, AND H. KROLL, *Am. Mineral.* **74**, 604 (1989).
16. I. PETROV. AND S. S. HAFNER, *Am. Mineral.* **73**, 97 (1988).
17. A. S. MARFUNIN, L. V. BERSHOV, M. L. MEILMAN, AND J. MICHOUPLIER, *Schweiz. Mineral. Petrogr. Mitt.* **47**, 13 (1967).